THE JOURNAL OF BIOLOGICAL CHEMISTRY VOL. 281, NO. 20, pp. 14207–14214, May 19, 2006

Quaternary Ammonium Compounds as Water Channel Blockers

*SPECIFICITY, POTENCY, AND SITE OF ACTION**

Received for publication, December 7, 2005, and in revised form, March 16, 2006 Published, JBC Papers in Press, March 21, 2006, DOI 10.1074/jbc.M513072200

Frank J. M. Detmers[‡], Bert L. de Groot[§], E. Matthias Müller[§], Andrew Hinton[¶], Irene B. M. Konings[‡], Mozes Sze[‡], Sabine L. Flitsch[¶1], Helmut Grubmüller[§], and Peter M. T. Deen[‡2]

From the [‡]Department of Physiology, Nijmegen Center for Molecular Life Sciences, Radboud University Nijmegen Medical Center, 6500 HB Nijmegen, Nijmegen, The Netherlands, the [§]Max-Planck Institute for Biophysical Chemistry, Theoretical and Computational Biophysics Department, Am Fassberg, D-37077, Göttingen, Germany, and the [¶]Department of Chemistry, University of Edinburgh, Kings Buildings, West Mains Road, EH9 3JJ Scotland, United Kingdom

Excessive water uptake through Aquaporins (AQP) can be life-threatening and reversible AQP inhibitors are needed. Here, we determined the specificity, potency, and binding site of tetraethylammonium (TEA) to block Aquaporin water permeability. Using oocytes, externally applied TEA blocked AQP1/AQP2/AQP4 with IC_{50} values of 1.4, 6.2, and 9.8 μM, respectively. Related tetraammonium compounds yielded some (propyl) or no (methyl, butyl, or pentyl) inhibition. TEA inhibition was lost upon a Tyr to Phe amino acid switch in the external water pore of AQP1/AQP2/AQP4, whereas the water permeability of AQP3 and AQP5, which lack a corresponding Tyr, was not blocked by TEA. Consistent with experimental data, multi-nanosecond molecular dynamics simulations showed one stable binding site for TEA, but not tetramethyl (TMA), in AQP1, resulting in a nearly 50% water permeability inhibition, which was reduced in AQP1-Y186F due to effects on the TEA inhibitory binding region. Moreover, in the simulation TEA interacted with charged residues in the C (Asp^{128}) and E (Asp^{185}) loop, and the A(Tyr^{37}-Asn^{42}-Thr^{44}) loop of the neighboring monomer, but not directly with Tyr^{186}. The loss of TEA inhibition in oocytes expressing properly folded AQP1-N42A or -T44A is in line with the computationally predicted binding mode. Our data reveal that the molecular interaction of TEA with AQP1 differs and is about 1000-fold more effective on AQPs than on potassium channels. Moreover, the observed experimental and simulated similarities open the way for rational design and virtual screening for AQP-specific inhibitors, with quaternary ammonium compounds in general, and TEA in particular as a lead compound.

Aquaporins form a large family of integral membrane proteins that facilitate specific, efficient, and passive permeation of water, whereas members of the aqua(glycero)porins also permeate small solutes, such as glycerol and urea (1). In mammals, 13 different aqua(glycero)porins have been identified, which differ in their tissues of expression, regulation, and selectivity. The gross structure of these membrane proteins is conserved and consists of six transmembrane domains with cytoplasmic N and C termini. The 1st intracellular (B) and 2nd extracellular (E) loop, both containing the highly conserved Asn-Pro-Ala (NPA) motive, fold back into the membrane and form the central part of the water pore (2, 3). Although every monomer is a functional water pore, aquaporins are expressed as homotetramers (4, 5). The atomic structures of human AQP1[3] (2) and GlpF from *Eschericia coli* (6), and real time molecular dynamics (MD) studies of these proteins (7, 8) established the molecular mechanism of water permeation.

Aquaporins are involved in the regulation of the water balance in many tissues (1, 9). In the kidney, AQP1 is present in the proximal tubules and thin descending limbs of Henle, in which almost 90% of the 180 liters of daily formed pro-urine is reabsorbed. The remaining volume is concentrated via the vasopressin-regulated AQP2, which is present in the apical membrane of principal cells of the renal collecting duct (10, 11), whereas AQP3 and AQP4, which are present in the basolateral membrane of these cells, form the exit pathway of water to the interstitium (1, 12). Besides the kidney, AQP3 is also found in the gastrointestinal tract and the stratum corneum of the skin, where it exhibits a high water permeability (13).

The clinical importance of AQPs is shown by their role in several disturbed water balance disorders, which can severely affect the quality of life and can be life threatening. The lack of AQP2 in states of excessive water loss is fundamental to widely occurring nephrogenic diabetes insipidus, a disease in which the kidney is unable to concentrate urine in response to vasopressin (1, 14). In mice, lack of AQP3 also results in an nephrogenic diabetes insipidus phenotype, indicating that AQP3 might also have an important role in urine concentration (15). AQP5 is present in the lung and exocrine glands, such as salivary and sweat glands (16), and the reduced saliva production in AQP5 knock-out mice underscores the important role of AQP5 in this process (17).

Paradoxically, disorders characterized by excessive water transport have also shown or have been ascribed to AQPs. AQP1 has been shown to be involved in tumor growth (18), and suggested to have a role in the development of pulmonary edema, eye glaucoma, and cyst formation in polycystic kidney disease (19). In several disorders, excessive renal water uptake is due to high renal plasma membrane AQP2 expression, which can lead to life threatening hyponatremia (20). AQP4 is, among other tissues, expressed in cells lining brain ventricles and has been shown to have a key role in the formation of brain edema (21), as a consequence of hyponatremia, stroke, accidents, and cancer.

Considering the important roles of AQPs in excessive water transport, reversible aquaporin-specific blockers are clinically highly desira-

* This work was supported by European Union Grants QLRT-2000-00778 (to S. L. F., H. G., and P. M. T. D.) and QLK3-CT-2001-00987 (to H. G. and P. M. T. D.) and a grant from the BBSRC (to S. L. F.). The costs of publication of this article were defrayed in part by the payment of page charges. This article must therefore be hereby marked "*advertisement*" in accordance with 18 U.S.C. Section 1734 solely to indicate this fact.

[1] School of Chemistry and Manchester Interdisciplinary Biocentre, 131 Princess St., Manchester M1 7ND, UK.

[2] To whom correspondence should be addressed: 286, Dept. of Physiology, RUNMC Nijmegen, P. O. Box 9101, 6500 HB Nijmegen, The Netherlands. Tel.: 31-243617347; Fax: 31-243616413; E-mail: p.deen@ncmls.ru.nl.

[3] The abbreviations used are: AQP, aquaporin; MD, molecular dynamics; TEA, tetraethylammonium; TMA, tetramethyl; WT, wild type; ER, endoplasmic reticulum.

ble. Such blockers for AQP1, AQP2, and AQP3 could serve well as diuretics and anti-tumor drugs (AQP1), whereas a timely administration of AQP4-specific blockers might reduce the formation of brain edema. Such blockers, however, are yet not available. Mercury, silver, and gold have been shown to inhibit AQPs (22, 23), but these metals are highly toxic and their inhibition is not reversible. Recently, however, it was reported that the ion channel blocker tetraethylammonium (TEA) weakly inhibits AQP1-mediated water permeability in oocytes (24) and mammalian cells (25). Because TEA can be chemically modified, it is potentially a promising lead compound for the development of AQP-specific and selective blockers. Therefore, we here tested its selectivity toward different water channels, determined its potency of inhibition on different AQPs, and determined the TEA-active site in AQP1, using a combination of an oocyte swelling assay, molecular docking, and MD simulations.

EXPERIMENTAL PROCEDURES

Constructs—Expression constructs encoding human (h) AQP1 (pXβg-ev1hAQP1; kind gift of Peter Agre (3)), pT$_7$T$_s$hAQP2 (10), or pBSKSI-IhAQP4 (26) were previously described. To generate pT7Ts-hAQP3, a 1444-bp BamHI-EcoRV fragment from pBSKSII hAQP3 (kind gift of Kenneth Ishibashi (27)) was cloned into the BglII/EcoRV sites of the oocyte expression vector pT7Ts (10). To obtain pT7Ts-hAQP5, an 887-bp BamHI/EcoRV fragment was cut from pBSKSII hAQP5 (kindly provided by Peter Agre (28)) and cloned into the BglII/EcoRV sites of pT7Ts. With the QuikChange site-directed mutagenesis kit (Stratagene, Heidelberg, Germany), mutations were introduced into the human AQP1–5 cDNA sequences, using the following forward primers: CTGGGCTTTAAATTCCCGGTG for Y37F, GGGAACGCCCAGACGGCGGTGCAGGAC for N42A, CAACCAGGCGGCGGTGCAGGAC for T44A, CGCAATTCCCTGGCTGATGGTGTCAAC for D128S, GCTATTTCCTACACCGGTTGTGGG for D185S, and GCTATTGACTTCACCGGTTGTGGGATTAACC for Y186F in AQP1; CCACCTCCTCGGGATCCATTTCACCGGCTGC for Y178F in AQP2; CATTGGCACCTCAATGGGCTTCTACTCCGGCTATGC for N209Y in AQP3; GCAATCAATTTTACCGGTGCCAGC for Y185F in AQP4; GGAATCTACTACACCGGTTGCTCCATGAAC for F179Y in AQP5; and GTCGGAATCTTCTACACCGGTTGCTCCATGAAC for Y178F/F179Y in AQP5. With these primers, restriction sites were introduced (DraI (Y37F), BsgI (N42A/T44A), HincII (D128S), and AgeI in AQP4-Y185F, AQP5-F179Y, and AQP5-Y178F/F179Y) or deleted (BstXI for AQP2-Y178F, NcoI site for AQP3-N209Y). Sequence analysis of selected clones confirmed that only the desired mutations were introduced.

Water Permeability Measurements—Expression constructs were linearized with SalI (pT7TshAQP2, pT7TshAQP5), XbaI (pT7TshAQP3, pBSKSIIhAQP4), or PstI (pXβg-ev1hAQP1). G-capped cRNA transcripts were synthesized *in vitro* using T7 RNA polymerase (AQP2, -3, and -5) or T3 RNA polymerase (AQP1 and -4). Transcription, and the isolation, integrity checks, and determination of the concentration of the cRNAs was done as described (29). *Xenopus* oocytes were isolated and stored as described (30). The oocytes were injected with 0.2–0.5 ng of cRNA coding for AQP1–5 and 0.5–1.0 ng of cRNA for the described mutants. One day after injection the follicular membranes were removed, and 2 days after injection the water permeability (Pf $\pm$ S.E.; $N \geqq 8$; in μm/s) was measured using a standard swelling assay (10), except that here ND96P saline buffer (96 mM NaCl, 2 mM KCl, 1.8 mM $CaCl_2$, 2.5 mM sodium pyruvate, 5 mM HEPES, pH 7.6, 200 mosM ND96P) instead of modified Barth's solution was used, because the tested inhibitors were better soluble in ND96P. For the swelling assays, ND96P was diluted 10 times with Milli-Q water. To test TEA-like compounds for their inhibitory activity, injected oocytes were pretreated with the compound in ND96P for 15 min after which they were subjected to a swelling assay in 20 mosM ND96P in the presence of the compound. Similar results were obtained without the preincubation step. The data shown are an average of five experiments (with 5 different batches of oocytes) in which 10 to 12 oocytes were tested at every condition. The Pf values under different conditions were compared within one batch of oocytes. The measured Pf values were statistically analyzed in an unpaired Student's *t* test. p values < 0.05 were considered significantly different. For the calculation of the IC_{50} values of potential blockers, the ratio of inhibition (I/I_0) was determined, in which "I" is the Pf at a certain inhibitor concentration and I_0 is the Pf in the absence of inhibitor. Both values are corrected for the Pf of non-injected oocytes. The I/I_0 values of each individual experiment were plotted against corresponding TEA concentrations and subjected to the automatic curve-fitting procedure in Microsoft Excel. The $IC_{50} \pm$ S.E. values were calculated from four independent experiments.

Membrane Isolation and Immunoblotting—Total membranes and plasma membranes were isolated from at least 8 oocytes per sample as described (31). Protein samples were denatured by incubation for 30 min at 37 °C in Laemmli buffer and blotted as described (29). Next, the blots were incubated overnight with 1:600 diluted mouse α-AQP1 (32), 1:1500 diluted rabbit α-AQP2 (29), or 1:500 diluted α-AQP4 (33) in TBST buffer (20 mM Tris, 140 mM NaCl, 0.1% Tween, pH 7.6) supplemented with 1% nonfat dried milk. As secondary antibodies, a 1:5000 dilution of goat α-rabbit IgG (Sigma) for AQP2 and AQP4, or a 1:2000 dilution of sheep α-mouse IgG (Sigma) for AQP1, both coupled to horseradish peroxidase, were used. Finally, AQP proteins were visualized using enhanced chemiluminescence (Pierce).

Determination of TEA Docking Sites—The molecular docking package DOCK 4.0 (34) was used to dock TEA into the x-ray structure of bovine AQP1 (Protein Data Bank code 1J4N). Atomic coordinates including hydrogen atoms and charge information for TEA were generated using the SYBYL package from Tripos Inc. (SYBYL 6.9, Tripos Inc., St. Louis, MI). A three-dimensional model of TEA was build using the CONCORD (57) package. Using the SPHGEN program (35), clusters of overlapping spheres were created in the upper vestibule of bovine AQP1. The original SPHGEN output file was edited using the InsightII package (58) until a cluster of 16 spheres remained that filled the solvent accessible surface area of AQP1. Hydrogens were added to the protein and charged using a Gasteiger-Hückel potential. The Dock package flexibly orientated the TEA molecule within the defined docking region, scoring and ranking the 100 best orientations. Orientations were ranked using the energy score of DOCK. The molecular visualization package WITNOTP (59) was used to inspect TEA in the upper vestibule of AQP1. Four representative orientations of TEA were selected as starting positions for subsequent MD studies.

Molecular Dynamics Simulations—MD simulations were started from the bovine AQP1 x-ray structure (PDB code 1J4N (36)), after modifying the structure to adopt the sequence of human AQP1. The 21 mutations and the insertion of 2 residues were carried out using the WHAT IF package (37). The percentage of sequence identity is 90.63%. None of the mutations or insertions is located in the pore region. AQP1 was simulated as a tetramer embedded in a solvated palmitoyloleoyl phosphatidylethanolamine lipid bilayer. The simulation system contained 8,340 protein atoms, 14,093 lipid atoms, 19,769 SPC water molecules (38), and four chloride ions, resulting in a system size of 81,739 atoms. The simulation setup and conditions were identical to those described before (7). In short, MD simulations were carried out using the Gromacs simulation suite (39). Lincs and Settle (40, 41) were applied

to constrain covalent bond lengths, allowing an integration time step of 2 fs. Electrostatic interactions were calculated using the Particle-Mesh Ewald method (40). The temperature was kept constant by separately coupling (τ = 0.1 ps) the protein, lipids, and solvent to an external temperature bath (42). The pressure was kept constant by weak coupling (τ = 1.0 ps) in the z-direction (normal to the bilayer plane) to a pressure bath (42). The gromacs force field was applied, which is the gromos 87 force field (43) with slight modifications (44) and explicit hydrogens on aromatic residues. To equilibrate the system, 500 ps of MD were performed with harmonic position restraints on all non-hydrogen protein atoms (k = 1000 kJ/(mol nm)). All subsequent simulations started from the resulting structure.

In total, seven simulations were performed, five of the wild type protein (WT), and two of the Y186F mutant. The simulation length of the seven production runs was 15 ns for each of the simulations, totaling 105 ns of simulation time. For the simulations including TEA and tetramethyl (TMA), initial positions for the inhibitors were derived from the docking approach described above. For WT_TEA1, TEA was placed at four different docking positions within the four monomeric channels of the tetramer, respectively (for the selection procedure of the docking orientations, see above). After inserting the TEA molecules, those water molecules that showed significant overlap with the inhibitor were removed from the simulation system. Because in this simulation TEA remained stably bound to the protein only in one of the four positions (see also "Results"), a second simulation (WT_TEA2) was started with TEA molecules bound to this position in all four monomers. In both simulations, to re-equilibrate the system, the position of the central nitrogen atom of the TEA was kept fixed by a harmonic positional restraint (k = 10000 kJ/(mol nm)) for 500 ps. The third simulation including TEA (WT_TEA3) started from the same conformation as WT_TEA2, but the equilibration period was extended to 3 ns before the production phase started. The WT_TMA simulation started, like the WT_TEA1 simulation, with TMA bound to four different positions obtained from the docking study described above. To all simulation systems including TEA and TMA, four additional chloride ions were added to compensate for the net charge of the quaternary ammonium ions.

The starting structures for the simulations of the Y186F mutant, Y186F_free and Y186F_TEA, were modeled from the structures, after equilibration, of the WT_free and WT_TEA3 simulation, respectively, by replacing the tyrosine hydroxide groups by a proton. Free energy changes associated with the Y186F mutation were estimated with thermodynamic integration calculations. The difference in stability between the WT and mutant protein was estimated from the free energy difference between the mutation in the folded protein and in a model of the unfolded state (modeled as a tripeptide in solution). All thermodynamic integration simulations were carried out using the method of slow growth (45), *i.e.* by gradually introducing the mutation into the simulated system (using soft-core parameters $\alpha = 0$ (resulting in linear interpolation of the non-bonded interactions) and σ = 0.3 nm) during a simulation period of 1 ns. For both the folded state and unfolded state (tripeptide), forward and backward mutations were simulated to ensure that the mutation was sufficiently reversible and hysteresis effects were small. For molecular visualization the pymol program (46) was used.

RESULTS

Quaternary Ammonium Compounds Tested on Human AQP1—Brooks *et al.* (24) recently reported that 100 μM TEA could reversibly inhibit water permeation through AQP1. To test whether we could reproduce these data, *Xenopus* oocytes were injected with 0.2 ng of AQP1 cRNA and tested in an oocyte-swelling assay in the presence or absence of 100 μM TEA. Oocytes treated with TEA showed a reduced Pf of 44 ± 14% compared with controls (Fig. 1*A*). After subjection to a swelling assay in the presence of TEA, oocytes were washed four times and allowed to recover to the normal volume for 4 h. Subsequent analysis of these oocytes in a swelling assay in the absence of TEA (Fig. 1*A*, *wash*) revealed a Pf that was significantly higher than when they were treated with TEA (p = 0.038), and which was not significantly different from AQP1-expressing control oocytes (p = 0.074). These data confirm that the water permeation through AQP1 can be reversibly inhibited by TEA.

To determine whether the lengths of the carbon side chain of quaternary ammonium compounds affected the inhibition of AQP1 water permeability, 100 μM concentrations of TMA-, tetrapropyl- (TPrA), tetrabutyl- (TBA), and tetrapentyl (TPeA) ammonium compounds were tested on AQP1-expressing oocytes. Determination of the Pfs revealed that, besides TEA, only TPrA significantly inhibited the AQP1 water permeability (32 ± 15%; p = 0.027; Fig. 1*B*). The inhibition by

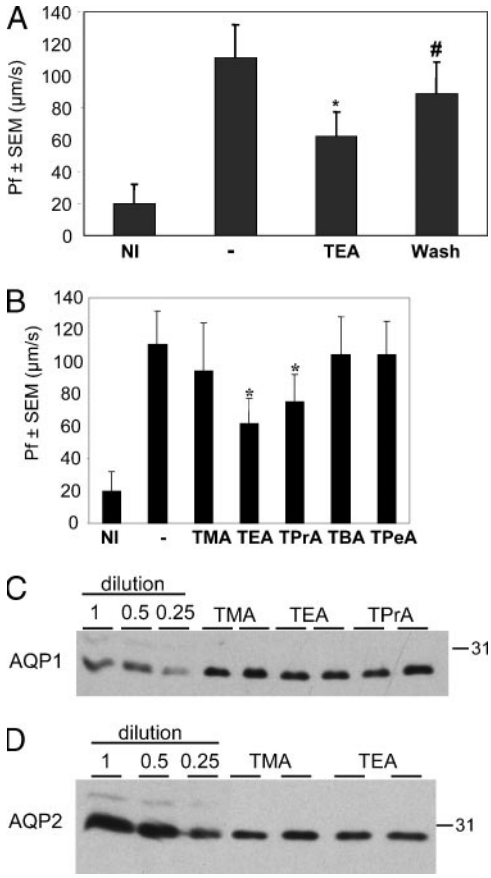

FIGURE 1. **Inhibition of the water permeability of AQP1-expressing oocytes by quaternary ammonium compounds.** *A*, reversibility of inhibition by TEA. Treatment of AQP1-expressing oocytes with 100 μM TEA results in a 44 ± 14% reduction of the water permeability compared with untreated oocytes. After extensive washing (indicated) and 4 h recovery of the oocytes, determination of the water permeability revealed a significantly higher Pf compared with the TEA-treated oocytes; *NI*, non-injected controls; −, without inhibitor; *, p = 0.014; #, p = 0.038. *B*, selectivity of AQP1 inhibition. AQP1-expressing oocytes were incubated with 100 μM quaternary ammonium salts with methyl (TMA), ethyl (TEA), propyl (TPrA), butyl (TBA), or pentyl (TPeA) carbon side chains and subjected to a standard swelling assay. Besides TEA, also TPrA showed a significant inhibition of the water permeability; *, $p < 0.03$. *C* and *D*, TEA and TPrA do not affect AQP expression in the oolemma. Immunoblots of plasma membrane equivalents of AQP1 (*C*) and AQP2 (*D*) expressing oocytes, isolated after incubation for 15 min with 100 μM TMA, TEA, or TPrA (indicated), revealed similar expression levels. A 2-fold dilution series of oocytes expressing each was blotted in parallel.

TPrA was not significantly different from that of TEA and was thus as effective as TEA at the tested concentration of 100 μM.

In principle, the effect of TEA and TPrA on AQP1 water permeation could be either a direct effect of the compound on AQP1 functioning or a result of a reduced plasma membrane expression of AQP1 in the presence of the blockers. To address this question, AQP1-expressing oocytes were incubated with 100 μM TMA, TEA, or TPrA for 15 min, after which plasma membranes were isolated from eight oocytes in duplicate and immunoblotted for AQP1 (Fig. 1*C*). Analysis of the immunoblot signals revealed similar plasma membrane expression of AQP1 for oocytes treated with TEA/TPrA *versus* TMA ($p = 0.11/0.20$ respectively; $n = 4$). As differences in AQP1 amounts revealed different signal intensities at this exposure time (dilution series), this indicated that the reduced water permeability with TEA or TPrA was due to a direct inhibition of AQP1 instead of effects on the levels of AQP1 plasma membrane expression.

Screening of AQP2–5 for Inhibitory Effects of Quaternary Ammonium Compounds—To determine whether the quaternary ammonium compounds specifically inhibit AQP1 or also affect the water permeation of other AQPs, oocytes expressing human AQP2, AQP3, AQP4, or AQP5 were subjected to swelling assays in the presence or absence of 100 μM TMA, TEA, TPrA, TBA, or TPeA. Determination of the Pfs revealed that, besides AQP1, the water permeability of AQP2 and AQP4 was inhibited by TEA to 49 ± 15 and 55 ± 18%, respectively (data not shown). In addition, the other four ammonium compounds did not have a significant inhibitory effect on the water permeability of AQP2 or AQP4, and the water permeability of AQP3 or AQP5 was not inhibited by any of the compounds tested (data not shown).

The AQP1 inhibitors TEA and TPrA did not affect AQP1 plasma membrane expression (Fig. 1*C*). To test whether the same holds for AQP2, oocytes expressing AQP2 were incubated with TMA or TEA and plasma membranes were isolated as above. Subsequent immunoblotting for AQP2 revealed similar AQP2 plasma membrane expression levels for oocytes treated with TMA *versus* TEA ($p = 0.34$; $n = 4$; Fig. 1*D*), which indicated that TEA also directly affects AQP2 water permeability, instead of reducing its expression in the oolemma.

Potency of TEA to Inhibit AQP1, -2, and -4 Water Permeation—As shown in Fig. 1*B*, the level of water permeability inhibition through AQP1 was similar for TEA and TPrA at 100 μM concentration. To determine the potency of each compound, AQP1-expressing oocytes were subjected to swelling assays in the absence or presence of 4 or 100 μM of each inhibitor. Determination of the Pf revealed that the inhibition with 4 μM TEA (42 ± 11%) was high and not significantly different from that of 100 μM TEA (40 ± 14%; Fig. 2*A*). In contrast, no significant inhibition was observed with 4 μM TPrA, whereas 100 μM TPrA again showed a significant inhibition of 29 ± 12%. This indicates that the potency of TEA to inhibit AQP1 water permeation is higher than of TPrA.

TEA inhibited the water permeability of AQP1, AQP2, and AQP4. To determine the potency of TEA for these different AQPs, oocytes expressing each AQP were subjected to swelling assays with different concentrations of TEA to determine the IC_{50} values for AQP1, -2, and -4 (Fig. 2*B*). Interestingly, AQP1, AQP2, and AQP4 appeared to have different IC_{50} values for TEA. For AQP1, a 46% inhibition of the water permeability was already observed at 4 μM TEA, which was not further increased for concentrations up to 100 μM or above (Fig. 2*B*). The obtained IC_{50} value of TEA for AQP1 appeared to be 1.4 ± 0.8 μM. The observed IC_{50} values for AQP2 and AQP4 were 6.2 ± 1.9 and 9.8 ± 2.3 μM, respectively, whereas the maximum level of inhibition by TEA was 40 ± 12% for AQP2 and 57 ± 9% for AQP4. These results indicated that the potency of TEA to inhibit water permeation through AQP1 is 4–6 times higher than for AQP2 or AQP4.

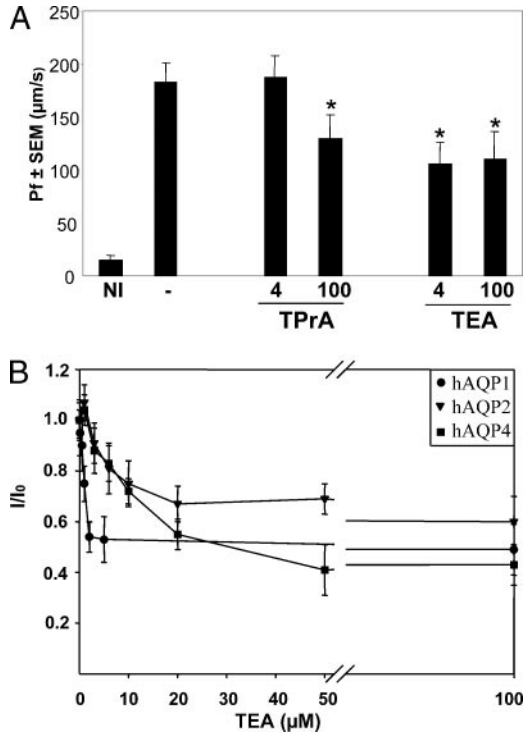

FIGURE 2. **The potency of TEA and TPrA to inhibit AQP1, -2, and -4 water permeation.** *A*, potency of AQP1 inhibitors. Water permeabilities (Pf) of AQP1-expressing oocytes incubated with 4 or 100 μM tetraethylammonium or tetrapropylammonium (TPrA). TEA was fully inhibited at both concentrations, whereas no significant inhibition was observed for 4 μM TprA; *NI*, non-injected control; −, without inhibitor; *, $p < 0.02$. *B*, determination of the IC_{50} concentrations. AQP1-, AQP2-, or AQP4-expressing oocytes were incubated with different concentrations of TEA and subjected to a standard swelling assay. The IC_{50} value of TEA for AQP1 (●) is 1.4 ± 0.8 μM, for AQP2 (▼), 6.2 ± 1.9 μM; and for AQP4 (■), 9.8 ± 2.3 μM.

The Involvement of a Tyrosine Residue in the E-loop for TEA Inhibition—The water permeation of AQP1-Y186F, in which Tyr^{186} in the E-loop is replaced by Phe, was no longer sensitive to TEA, which indicated an involvement of Tyr^{186} in binding TEA (24). Interestingly, an alignment of the amino acid sequences of the E-loop of human AQP1, -2, -3, -4, and -5 shows that Tyr^{186} is conserved in AQP1, -2, and -4 (Fig. 3*A*), which are all inhibited by TEA. In contrast, AQP3 and AQP5, which are not inhibited by TEA, have Asn and Phe residues at this position, respectively.

To further explore an involvement of this Tyr in the inhibition of water permeation by TEA, Tyr^{186} in hAQP1, Tyr^{178} in hAQP2, and Tyr^{185} in hAQP4 were replaced by Phe. Introduction of amino acid changes in AQP1–4 can result in their misfolding, which will lead to a predominant retention in the endoplasmic reticulum (ER) and immunoblot detection of high mannose-glycosylated AQP1/2/4 of around 32 kDa (14, 47–49). To avoid working with such proteins, because we cannot be confident about their proper structure, total membranes of oocytes expressing the WT and mutant AQPs 1, 2, or 4 were subjected to immunoblot analysis. In contrast to the ER-retained AQP2 mutant control, AQP2-T126M (49), a 32-kDa band was not observed for any of the AQP1/2/4 mutants (Fig. 3*B*), indicating their proper folding. Subsequent analysis of their water permeability in the presence or absence of 100 μM TEA revealed that AQP1-Y186F, AQP2-Y178F, and AQP4-Y185F were functional water channels, which showed no statistically significant inhibition by TEA anymore (Fig. 3*C*).

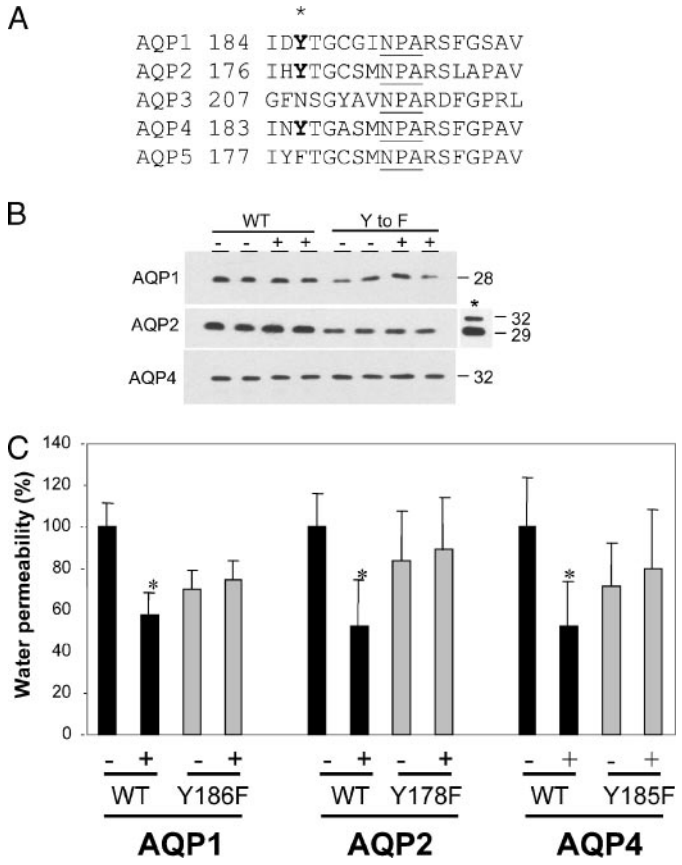

FIGURE 3. **The role of E-loop tyrosine residues in TEA-mediated inhibition of the water permeability of AQP1–5.** *A*, amino acid alignment of the E-loops of human AQP1–5. The conserved NPA box is *underlined*, *, indicates the tyrosine residue that is conserved in the TEA-sensitive water channels. *B*, expression forms of wild-type and Tyr to Phe mutants of AQP1, -2, and -4. Immunoblots of total membrane equivalents of oocytes expressing wild type or Tyr to Phe mutant proteins of AQP1, -2, and -4 treated with (+) or without (−) TEA revealed only 29-kDa proteins, which indicated that the mutant proteins are properly folded. The *inset* marked with an *asterisk* shows a typical example of an ER-retarded AQP2 mutant (AQP2-T126M), which, besides the 29-kDa band, also shows the high mannose-glycosylated band of 32 kDa. *C*, the role of E-loop tyrosines in TEA-inhibited water permeation. The water permeabilities of oocytes expressing WT-AQP1, -2, or -4 or their Tyr to Phe mutants were measured in the absence (−) or presence (+) of 100 μM TEA. The permeabilities are expressed in % related to untreated oocytes expressing the WT-AQPs. The water permeabilities of oocytes expressing WT-AQP1, -AQP2, or -AQP4 were inhibited 42 ± 11 ($p = 0.008$), 48 ± 23 ($p = 0.021$), or 47 ± 22% ($p = 0.026$), respectively.

To investigate whether introduction of a Tyr at a corresponding position in AQP3 or AQP5 would result in TEA-sensitive water permeability, mutants were made in which a tyrosine was exchanged for Asn^{209} in AQP3 and Phe^{179} in AQP5. Because AQP5 has a Tyr residue at position 178, another AQP5 mutant was made in which residues 178 and 179 were swapped (*i.e.* Tyr^{178}/Phe^{179} changed into Phe^{178}/Tyr^{179}). Subsequent immunoblot and swelling assays of the encoded proteins showed that none of the AQP3/5 mutants was misfolded and that they formed functional channels, which were not significantly inhibited by TEA (data not shown).

Together, these data indicated that the loss of swelling inhibition by TEA in AQP1, AQP2, and AQP4 is only because of the Tyr to Phe mutations, but that the introduction of a Tyr residue at the corresponding sites in AQP3/5 did not result in TEA-sensitive water permeability.

Molecular Docking of TEA—To identify the binding site of TEA in AQP1, TEA was subjected to docking studies in the upper vestibule of AQP1. Analysis of the obtained data revealed that TEA was able to move freely within the defined docking region. Of the 100 best scored orientations, the majority of TEA orientations showed little bias to any specific group of AQP1 residues. Four representative AQP1-TEA starting orientations generated by DOCK were selected for subsequent MD simulations. These docked TEA orientations satisfied basic steric and electrostatic considerations and were chosen to be as spatially distinct from each other as possible.

Molecular Dynamics Simulations of AQP1 Inhibition by TEA—Fig. 4*a* shows the four initial positions of TEA, one in each monomer, obtained from the docking study, which formed the starting structure of simulation WT_TEA1. In this simulation, only one TEA stayed bound during the 15-ns simulation time. To better characterize this binding site, and to obtain better statistics, TEA was placed at this position in all four monomers, and two subsequent simulations were carried out, differing from each other in the relaxation time (500 ps for WT_TEA2 and 3 ns for WT_TEA3). In WT_TEA2 only one TEA stayed bound during the 15-ns simulation time, whereas in WT_TEA3 all four TEA remained bound. This striking difference suggests that induced-fit relaxation motions do occur at a nanosecond time scale and likely affect the AQP1-TEA interactions. In contrast, TMA did not bind in any of the four positions studied, which is in agreement with the results from swelling assays (Fig. 1*B*). In Y186F_TEA, two TEA molecules stayed bound during the 15-ns simulation time.

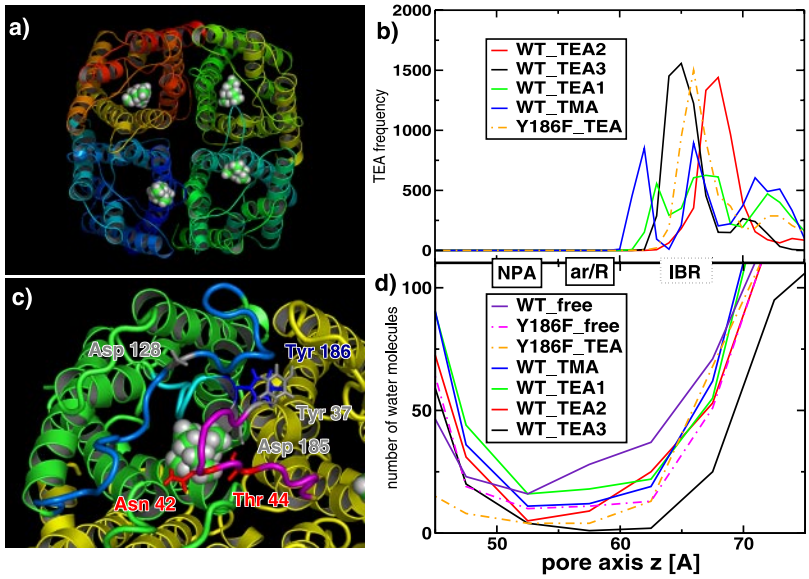

FIGURE 4. **Molecular dynamics simulations on TEA binding to AQP1.** *a*, starting configurations for the MD simulations described in the text. TEA molecules (space-filling representation) at four representative TEA positions out of 100 nearly equally scored docking results were included. *b*, histogram of the nitrogen atom positions for the quaternary ammonium ions as a function of the pore axis. The WT_TEA3 simulations have been used to define the inhibitor binding region (*IBR*). *c*, representative snapshot of the TEA binding site. TEA is embedded in a pocket built by the C-loop (*marine*), and E-loop (*cyan*) of one and the A-loop (*magenta*) of the neighboring monomer. Mutations to validate the predicted binding site are represented as *sticks* (*red* for the properly folded and *gray* for the others). *d*, effect of inhibitor binding on water mobility in the pore: the number of water molecules that pass 0.5-nm thick slices during the MD simulations as a function of the pore axis. The water flux in simulation for WT_TEA3 in the NPA, aromatic arginine (ar/R), and the IBR region is lower than in the mutant and the inhibitor simulations.

Fig. 4*b* shows histograms of TEA positions along the pore axis *z*. Because all four TEA molecules remained bound during the 15-ns simulation time, WT_TEA3 (*black curve*) was used to define an inhibitor binding region between 63 and 67 Å along the pore axis *z*. The shape of the WT_TEA2 curve (*red*) is similar to the one of WT_TEA3, but is shifted by about 4 Å toward the extracellular surface, indicating that the unbound TEA molecules stayed close to the protein surface. Visual inspection of the trajectory showed that one TEA bound to the central pore of the tetramer and not at the pore entry sites. In WT_TEA1 (*green*) the curve is wider because of the different starting positions and the fast unbinding of TEA from the three unstable positions. No TMA molecule bound to AQP1, as reflected in the wide density profile in the pore axis *z* of WT_TMA (*blue*). Remarkably, the sharp peak of Y186F_TEA (*orange*) is shifted by about 1 Å toward the extracellular surface, *i.e.* the two TEA molecules bound at positions located slightly toward the outside of the pore as compared with the WT.

The six monomers (from different simulations) in which TEA remained bound were used to characterize the interactions with the binding site. As shown in a representative snapshot (Fig. 4*c*) the binding site contains contributions from the C- (*marine*) and E-loops (*cyan*). Additionally, in the simulation the A-loop (*magenta*) of the neighboring monomer covered the binding site much like a lid, which suggests an important role in TEA binding. In our simulations, Tyr^{186} formed no direct contacts to TEA.

To study the influence of the TEA on water permeability, we counted the number of water molecules passing slices (of 5 Å thickness each) of the pore during the simulations (Fig. 4*d*). In these curves, the point of lowest mobility is expected to dominate the overall permeability. As can be seen, the water permeability is significantly larger in WT_free (*purple*) than, *e.g.* in the WT_TEA3 simulation, where all four TEA molecules stayed bound. This effect is particularly pronounced in the TEA binding region, where the water flux through the 5-Å thick layers in WT_free is 10–15 times higher than in WT_TEA3. These results strongly suggest that the water permeability of AQP1 is indeed significantly reduced by the binding of TEA.

To study why Y186F changes the inhibitory activity of TEA on AQP1 despite the fact that it is not located directly at the putative binding site (see Fig. 4*d*), we performed thermodynamic integration simulations for this mutation. The obtained relatively small free energy difference of $\Delta\Delta G = 20$ kJ/mol between the WT and the mutant suggests that the mutant leaves the protein structure mostly intact and, therefore the model provides a reliable basis for subsequent molecular dynamics simulations. Accordingly, we performed two 15-ns MD simulations of the mutant with and without bound TEA. The water flux analysis (Fig. 4*d*) of the mutant without TEA (Y186F_free, *dotted magenta curve*) and with TEA (Y186F_TEA, *dotted orange curve*) show a much smaller TEA effect than observed for wild-type AQP1, which is in full agreement with the oocyte measurements.

Exploring the Putative TEA-binding Sites in AQP1—The molecular dynamics simulations provided a model for the binding mode of TEA. To validate this prediction, *in vitro* mutagenesis was employed to change the residues interacting with TEA (Y37F, N42A, T44A, D128S, and D185S). Expression in oocytes revealed that AQP1-N42A, AQP1-T44A, and WT-AQP1 were mainly expressed as 28-kDa bands, whereas all others showed strong ER-glycosylation forms, indicating that these latter proteins are not properly folded (Fig. 5*A*). However, N42A and T44A eliminate the AQP1 *N*-glycosylation consensus site (50) and, therefore, analysis of their glycosylation state is not informative on their proper folding. Therefore, we analyzed their ratio of plasma membrane *versus* total membrane expression, as this is strongly reduced with improperly folded AQPs (31, 51). Immunoblot analysis, however, revealed that this ratio was not significantly different compared with WT-AQP1 (not shown). These data indicate that AQP1-N42A and T44A are properly folded and underscore findings obtained with AQP1-N42Q and AQP2-N123Q that glycosylation is not required for folding, oligomerization, cell surface expression, and function of AQPs in oocytes (50, 52). Subsequent swelling assays of the properly folded proteins revealed that the water permeability of WT-AQP1, but not of AQP1-N42A or AQP1-T44A, was inhibited by TEA (Fig. 5*B*).

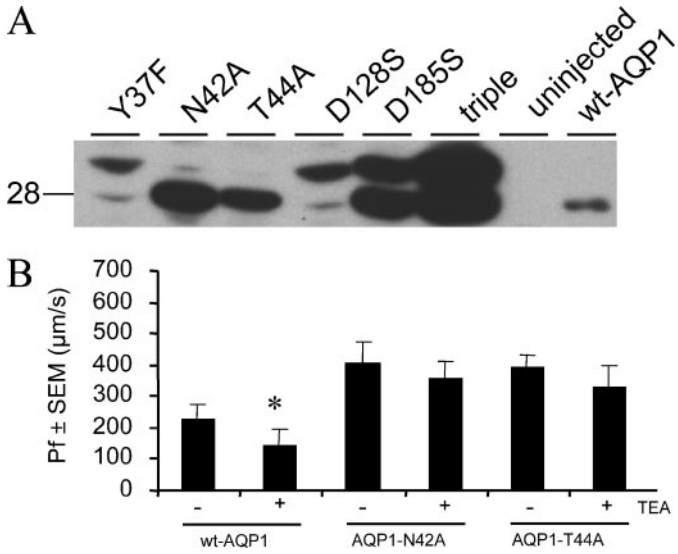

FIGURE 5. **Functional analysis of putative TEA binding sites in AQP1.** *A*, human WT-AQP1 or its mutants encoding Y37F, N42A, T44A, D128S, D185S, or the Y37F/D128S/D185S triple mutant were expressed in oocytes and analyzed for expression by immunoblotting. Except for WT-AQP1, and its N42A and T44A mutants, all mutant proteins revealed a 30-kDa band, besides the 28-kDa band, indicating to ER retention and misfolding. Molecular mass is indicated on the *left* in kDa. *B*, water permeabilities (Pf) of oocytes expressing WT-AQP1, AQP1-N42A, or AQP1-T44A in the presence or absence of 100 μM TEA. *, $p < 0.05$.

DISCUSSION

TEA Potently and Reversibly Inhibits Water Permeation through AQP1—We found that TEA reversibly inhibited AQP1 water permeation, in agreement with earlier findings (24). The unchanged plasma membrane expression levels in our studies of AQP1 (and AQP2) in oocytes treated with or without TEA, furthermore, indicated that the observed inhibitory effect is because of a direct effect on the particular AQP. This finding is corroborated by the absence of any effect of TEA on the water permeation conferred by AQP3, AQP5, and their E-loop tyrosine mutants (Fig. 3).

Compared with the results reported by Brooks *et al.* (24) the levels of AQP1 inhibition were considerably higher in our experiments. Whereas Brooks *et al.* (24) observed a 30% inhibition with 100 μM TEA and a significant inhibition at 50 μM or higher, we found a maximal level of nearly 50% inhibition for 4–100 μM TEA and an IC_{50} of around 1.4 μM. Similarly, whereas Brooks *et al.* (24) did not observe any inhibition of the AQP1 water permeation by TPrA, we found a significant 32% inhibition with this compound (Fig. 1). These differences might be due to the higher amounts of AQP1 cRNA injected by Brooks *et al.* (24) or, possibly, the apparent high variability in Pfs in their experiments (33–60%).

TEA Also Inhibits AQP2 and AQP4 Water Permeation—Besides AQP1, TEA also inhibits water permeation through AQP2 and AQP4, whereas the water permeabilities of oocytes expressing AQP3 or AQP5 were not affected. Although TEA could act on any part of the AQP protein, the convincing evidence that the E-loop forms the extracellular

face of the water pore (2, 3) and the loss of TEA inhibition with the E-loop Tyr to Phe mutants of AQP1, AQP2, and AQP4 strongly indicated that the binding site for TEA is in the vicinity of the E-loop (see also below). Similar to AQP1, inhibition by TEA leveled off for AQP2 and AQP4, although here at nearly 40 and 60% inhibition, respectively (Fig. 2*B*). The IC_{50} value for AQP1, however, was considerably lower than for AQP2 or AQP4 (1.4 μM *versus* 6.2 and 9.8, respectively), which shows that TEA is a more potent inhibitor of AQP1. This suggests that, although the E-loops of the water-selective channels AQP1, -2, and -4 are quite homologous, their vestibules do differ. This is underscored by our finding that TPrA does inhibit water permeation in AQP1, but not in AQP2 or AQP4. Assuming a similar mode of action as for TEA, the inhibition of AQP1 by TPrA, but not by TMA, TbuA, or TPeA, indicates that indeed specifically designed TEA derivatives may prove to be potential specific AQP blockers.

Several Residues Constitute the TEA Binding Site in AQP1—Water and potassium channels appear to share several features, although they are evolutionary distinct. Similar to AQPs, many potassium channels are homotetramers of 6 (and sometimes 2) α-helical transmembrane domains of which the last two are involved in the formation of the K^+-selective pore, which is about 3 Å at its narrowest point (53, 54). In potassium channels, aromatic residues at the extracellular mouth of the selectivity filter are thought to mediate binding to TEA (55, 56). Similarly, it has been suggested that Tyr^{186} in AQP1 is involved in TEA binding (24). Indeed, AQP1, AQP2, and AQP4, which all have a Tyr at a similar position, were inhibited by TEA, whereas AQPs that had a Tyr residue at another distance from the NPA box (AQP5) or had no Tyr residue at all in its E-loop (AQP3) were not inhibited by TEA. Also, the Tyr to Phe mutants of AQP1, AQP2, and AQP4, which were functional water channels, lacked inhibition by TEA (Fig. 3). All these mutants were properly folded, as judged by the absence of ER-glycosylated forms with immunoblot analyses (Fig. 3*C*) as well as by our thermodynamic integration simulations, which suggested that the Y186F mutation does not significantly destabilize the protein structure. This latter conclusion is corroborated by free molecular dynamics simulations of the mutant, which did not exhibit significant structural changes (simulation Y186F_free; Fig. 4).

The experiments above, however, do not exclude the possibility that TEA binds to residues other than Tyr^{186} and that the loss of inhibition by TEA with the Tyr to Phe mutations is because of other structural changes in AQP1. Although not conclusive, the fact that introducing a Tyr residue at the corresponding position does not introduce sensitivity to TEA in AQP3/AQP5 indicates that a Tyr at that position alone is not sufficient for TEA sensitivity. Also, the particular Tyr residue in AQP1 is located at the rim of the water pore (Fig. 4), which is relatively far from the AQP1 water pore aromatic arginine region (ar/R) and suggested that this residue may indirectly affect TEA affinity. Indeed, our simulations indicate that the binding site is mainly formed by amino acids located in A-loop (Tyr^{37}, Asn^{42}, Thr^{44}, and Asp^{48}), C-loop (Asp^{128}), and E-loop (Asp^{185}), whereas Tyr^{186} is not directly involved in TEA binding. Instead, the Y186F mutation seems to influence the structural flexibility of parts of the protein, especially the A-loop (simulation Y186F_TEA). The lack of water permeability inhibition by TEA mediated by the properly folded AQP1-N42A and AQP1-T44A proteins underscores the role of these residues in inhibitor binding. Intriguingly, however, Asn^{42} and Thr^{44} are essential for AQP1 glycosylation (50). Whether glycosylation may be involved in inhibitor binding and how the mutant Y186F changes the affinity of AQP1 for TEA will be the subject of future studies.

Our computational characterization of the binding site introduces a new viewpoint on TEA binding in AQP1. Up to now, studies in oocytes to investigate TEA binding modes only focused on mutations in the E-loop. Our simulations provide an extended picture of TEA binding. In particular, the A-loop of the neighboring monomer might function as a lid, which hinders TEA to leave the binding site. TEA, but not TMA, bound at this binding pocket, exhibits an inhibition that is of the same order of magnitude as that observed experimentally in oocytes.

In conclusion, we have shown that TEA shows a reversible and selective inhibition of water permeation through AQP1, AQP2, and AQP4 and that this inhibition is likely mediated through an interaction between TEA and amino acids located at the extracellular face of AQP1, especially the A-, C-, and E-loops. The IC_{50} values of TEA for AQP1, -2, and -4 are in the micromolar region (1.4, 6.2, and 9.4 μM), which indicates that quaternary ammonium compounds in general and TEA in particular are good lead compounds for the development of reversible and AQP-specific inhibitors in clinical applications. Moreover, the molecular characterization of the TEA binding site, corroborated by mutational studies, opens new perspectives for a rational structure-based approach to search for more efficient and selective blockers of different aquaporins.

Acknowledgments—We are indebted to Drs. Peter Agre, Johns Hopkins University, Baltimore, MD, and Kenneth Ishibashi, Department of Pharmacology, Jichi Medical School, Tochigi, Japan, for providing human AQP1/5 and AQP3 expression constructs, respectively.

REFERENCES

1. Nielsen, S., Frokiaer, J., Marples, D., Kwon, T. H., Agre, P., and Knepper, M. A. (2002) *Physiol. Rev.* **82,** 205–244
2. Murata, K., Mitsuoka, K., Hirai, T., Walz, T., Agre, P., Heymann, J. B., Engel, A., and Fujiyoshi, Y. (2000) *Nature* **407,** 599–605
3. Jung, J. S., Preston, G. M., Smith, B. L., Guggino, W. B., and Agre, P. (1994) *J. Biol. Chem.* **269,** 14648–14654
4. Van Hoek, A. N., Hom, M. L., Luthjens, L. H., de Jong, M. D., Dempster, J. A., and van Os, C. H. (1991) *J. Biol. Chem.* **266,** 16633–16635
5. Smith, B. L., and Agre, P. (1991) *J. Biol. Chem.* **266,** 6407–6415
6. Fu, D., Libson, A., Miercke, L. J., Weitzman, C., Nollert, P., Krucinski, J., and Stroud, R. M. (2000) *Science* **290,** 481–486
7. de Groot, B. L., and Grubmuller, H. (2001) *Science* **294,** 2353–2357
8. Tajkhorshid, E., Nollert, P., Jensen, M. O., Miercke, L. J., O'Connell, J., Stroud, R. M., and Schulten, K. (2002) *Science* **296,** 525–530
9. van Os, C. H., Kamsteeg, E. J., Marr, N., and Deen, P. M. T. (2000) *Pflugers Arch.* **440,** 513–520
10. Deen, P. M. T., Verdijk, M. A. J., Knoers, N. V. A. M., Wieringa, B., Monnens, L. A. H., van Os, C. H., and van Oost, B. A. (1994) *Science* **264,** 92–95
11. Fushimi, K., Uchida, S., Hara, Y., Hirata, Y., Marumo, F., and Sasaki, S. (1993) *Nature* **361,** 549–552
12. Deen, P. M. T., Van Balkom, B. W. M., and Kamsteeg, E. J. (2000) *Eur. J. Cell Biol.* **79,** 523–530
13. Sougrat, R., Morand, M., Gondran, C., Barre, P., Gobin, R., Bonte, F., Dumas, M., and Verbavatz, J. M. (2002) *J. Investig. Dermatol.* **118,** 678–685
14. Knoers, N. V. A. M., and Deen, P. M. T. (2001) *Pediatr. Nephrol.* **16,** 1146–1152
15. Ma, T., Song, Y., Yang, B., Gillespie, A., Carlson, E. J., Epstein, C. J., and Verkman, A. S. (2000) *Proc. Natl. Acad. Sci. U. S. A.* **97,** 4386–4391
16. Song, Y., Sonawane, N., and Verkman, A. S. (2002) *J. Physiol.* **541,** 561–568
17. Ma, T., Song, Y., Gillespie, A., Carlson, E. J., Epstein, C. J., and Verkman, A. S. (1999) *J. Biol. Chem.* **274,** 20071–20074
18. Saadoun, S., Papadopoulos, M. C., Hara-chikuma, M., and Verkman, A. S. (2005) *Nature* **434,** 786–792
19. King, L. S., and Agre, P. (1996) *Annu. Rev. Physiol.* **58,** 619–648
20. Pedersen, R. S., Bentzen, H., Bech, J. N., Nyvad, O., and Pedersen, E. B. (2003) *Kidney Int.* **63,** 1417–1425
21. Manley, G. T., Fujimura, M., Ma, T., Noshita, N., Filiz, F., Bollen, A. W., Chan, P., and Verkman, A. S. (2000) *Nat. Med.* **6,** 159–163
22. Preston, G. M., Jung, J. S., Guggino, W. B., and Agre, P. (1993) *J. Biol. Chem.* **268,** 17–20
23. Niemietz, C. M., and Tyerman, S. D. (2002) *FEBS Lett.* **531,** 443–447
24. Brooks, H. L., Regan, J. W., and Yool, A. J. (2000) *Mol. Pharmacol.* **57,** 1021–1026
25. Yool, A. J., Brokl, O. H., Pannabecker, T. L., Dantzler, W. H., and Stamer, W. D. (2002)

BMC Physiol. **2,** 4
26. Lu, M., Lee, M. D., Smith, B. L., Jung, J. S., Agre, P., Verdijk, M. A. J., Merkx, G., Rijss, J. P. L., and Deen, P. M. T. (1996) *Proc. Natl. Acad. Sci. U. S. A.* **93,** 10908–10912
27. Ishibashi, K., Sasaki, S., Fushimi, K., Uchida, S., Kuwahara, M., Saito, H., Furukawa, T., Nakajima, K., Yamaguchi, Y., and Gojobori, T. (1994) *Proc. Natl. Acad. Sci. U. S. A.* **91,** 6269–6273
28. Lee, M. D., Bhakta, K. Y., Raina, S., Yonescu, R., Griffin, C. A., Copeland, N. G., Gilbert, D. J., Jenkins, N. A., Preston, G. M., and Agre, P. (1996) *J. Biol. Chem.* **271,** 8599–8604
29. Deen, P. M. T., Croes, H., van Aubel, R. A., Ginsel, L. A., and van Os, C. H. (1995) *J. Clin. Investig.* **95,** 2291–2296
30. Mulders, S. M., Bichet, D. G., Rijss, J. P. L., Kamsteeg, E. J., Arthus, M. F., Lonergan, M., Fujiwara, M., Morgan, K., Leijendekker, R., van der Sluijs, P., van Os, C. H., and Deen, P. M. T. (1998) *J. Clin. Investig.* **102,** 57–66
31. Kamsteeg, E. J., and Deen, P. M. T. (2001) *Biochem. Biophys. Res. Commun.* **282,** 683–690
32. Deen, P. M. T., Nielsen, S., Bindels, R. J. M., and van Os, C. H. (1997) *Pflugers Arch.* **433,** 780–787
33. Van Balkom, B. W. M., Van Raak, M., Breton, S., Pastor-Soler, N., Bouley, R., van der Sluijs, P., Brown, D., and Deen, P. M. T. (2003) *J. Biol. Chem.* **278,** 1101–1107
34. Ewing, T. J., and Kuntz, I. D. (1997) *J. Comp. Chem.* **18,** 1175–1189
35. Kuntz, I. D., Blaney, J. M., Oatley, S. J., Langridge, R., and Ferrin, T. E. (1982) *J. Mol. Biol.* **161,** 269–288
36. Sui, H., Han, B. G., Lee, J. K., Walian, P., and Jap, B. K. (2001) *Nature* **414,** 872–878
37. Vriend, G. (1990) *J. Mol. Graph.* **8,** 52–56, 29
38. Berendsen, H. J., Postma, J. P., van Gunsteren, W. F., and Hermans, J. (2004) in *Intermolecular Forces* (Pullman, B., ed) D. Reidel Publishing Company, Dordrecht
39. Lindahl, E., Hess, B., and van der Spoel, D. (2001) *J. Mol. Model.* **7,** 306–317
40. Hess, B., Bekker, H., Berendsen, H. J., and Fraaije, J. G. (1997) *J. Comp. Chem.* **18,** 1463–1472
41. Miyamoto, S., and Kollman, P. A. (1992) *J. Comp. Chem.* **13,** 952–962
42. Berendsen, H. J., Postma, J. P., DiNola, A., and Haak, J. R. (1984) *J. Chem. Phys.* **81,** 3684–3690
43. van Gunsteren, W. F., and Berendsen, H. J. (1987) *GROMOS Manual, BIOMOS,* Biomolecular Software, Laboratory of Physical Chemistry, University of Groningen, The Netherlands
44. Van Buuren, A. R., Marrink, S.-J., and Berendsen, H. J. C. (1993) *J. Phys. Chem.* **97,** 9206–9212
45. Bash, P. A., Singh, U. C., Langridge, R., and Kollman, P. A. (1987) *Science* **236,** 564–568
46. DeLano, W. L. (2002) *The PyMOL Molecular Graphics System*, DeLano Scientific, San Carlos, CA
47. Mulders, S. M., van der Kemp, A. J., Terlouw, S. A., van Boxtel, H. A. F., van Os, C. H., and Deen, P. M. T. (1998) *Pflugers Arch.* **436,** 599–607
48. Marr, N., Bichet, D. G., Hoefs, S., Savelkoul, P. J., Konings, I. B., De Mattia, F., Graat, M. P., Arthus, M. F., Lonergan, M., Fujiwara, T. M., Knoers, N. V. A. M., Landau, D., Balfe, W. J., Oksche, A., Rosenthal, W., Muller, D., van Os, C. H., and Deen, P. M. T. (2002) *J. Am. Soc. Nephrol.* **13,** 2267–2277
49. Mulders, S. M., Knoers, N. V. A. M., van Lieburg, A. F., Monnens, L. A. H., Leumann, E., Wuhl, E., Schober, E., Rijss, J. P. L., van Os, C. H., and Deen, P. M. T. (1997) *J. Am. Soc. Nephrol.* **8,** 242–248
50. Preston, G. M., Jung, J. S., Guggino, W. B., and Agre, P. (1994) *J. Biol. Chem.* **269,** 1668–1673
51. Marr, N., Kamsteeg, E. J., Van Raak, M., van Os, C. H., and Deen, P. M. T. (2001) *Pflugers Arch.* **442,** 73–77
52. Hendriks, G., Koudijs, M., van Balkom, B. W., Oorschot, V., Klumperman, J., Deen, P. M. T., and van der Sluijs, P. (2004) *J. Biol. Chem.* **279,** 2975–2983
53. Blaustein, R. O., and Miller, C. (2004) *Nature* **427,** 499–500
54. Doyle, D. A., Morais, C. J., Pfuetzner, R. A., Kuo, A., Gulbis, J. M., Cohen, S. L., Chait, B. T., and MacKinnon, R. (1998) *Science* **280,** 69–77
55. MacKinnon, R., and Yellen, G. (1990) *Science* **250,** 276–279
56. Zhou, M., Morais-Cabral, J. H., Mann, S., and MacKinnon, R. (2001) *Nature* **411,** 657–661
57. Pearlman, R. S. (1998) *CONCORD User's Manual*, Tripos Inc., St. Louis, MO
58. Accelrys Inc. (2000) *InsightII Modeling Environment, Release 2000*, Accelrys Inc., San Diego, CA
59. Widmer, A. (1997) *WITNOTP: A Computer Program for Molecular Modeling*, Novartis, Basel, Switzerland